Malaysian Journal of Chemistry, 2025, Vol. 27(5), 110-120
(Special Issue: *5th IKMPB Online Symposium, IKMPB 2025*)

Crosslinking Effects on Swelling, Thermal and Physicochemical Properties of Hemicellulose-Based Hydrogels

Nurathirah Nabihah Sairi[1], Shariff Ibrahim[1,2], Noraini Hamzah[1,2], Norizan Ahmat[3], Mohammed Falalu Hamza[1], Wan Mohd Faizal Wan Ishak[4] and Sabiha Hanim Saleh[1,2]*

[1]Department of Chemistry and Environment, Faculty of Applied Sciences, Universiti Teknologi MARA, 40450 Shah Alam, Selangor, Malaysia

[2]Industrial Waste Conversion Technology Research Group, Faculty of Applied Sciences, Universiti Teknologi MARA, 40450 Shah Alam, Selangor, Malaysia

[3]Centre of Foundation Studies, Universiti Teknologi MARA, Cawangan Selangor, Kampus Dengkil, 43800 Dengkil, Selangor, Malaysia

[4]Faculty of Bioengineering and Technology, Universiti Malaysia Kelantan Kampus Jeli, Beg Berkunci No.100, 17600 Jeli, Kelantan, Malaysia

*Corresponding author (e-mail: sabihahanim@uitm.edu.my)

The structure, swelling behaviour, and stability of hydrogels derived from oil palm empty fruit bunches (OPEFB) hemicellulose are strongly influenced by the type and amount of crosslinkers used. This study investigates the effects of varying amounts of N,N'-methylene bisacrylamide (MBA) and glutaraldehyde (GA) on the swelling, physicochemical and thermal properties of hemicellulose-based hydrogels. Hemicellulose was extracted from OPEFB using microwave-assisted alkali treatment at 130°C for 30 minutes and was subsequently used to prepare hydrogel with different amounts of MBA and GA as crosslinking agents. The results demonstrated that hydrogels crosslinked with 0.01 g MBA exhibited the highest swelling ratio at 615%, attributed to the formation of dense and rigid network structures. In contrast, GA-crosslinked hydrogels achieved a swelling ratio of up to 1.64 (164%) and exhibited more balanced swelling behaviour, maintaining flexibility while ensuring structural stability. Field emission scanning electron microscopy showed a more uniform and dense network structure in MBA-crosslinked hydrogels. Furthermore, thermogravimetric analysis demonstrated enhanced thermal stability in the presence of MBA, with higher decomposition temperatures compared to GA-crosslinked samples. These findings highlight the greater effectiveness of MBA as a crosslinking agent in improving the properties of hemicellulose-based hydrogels, supporting their suitability for agricultural applications such as soil conditioners or controlled-release fertilisers.

Keywords: Oil palm empty fruit bunches; N, N'-methylene bisacrylamide; glutaraldehyde; crosslinking agent, hydrogel

Received: April 2025; Accepted: August 2025

Oil palm empty fruit bunches (OPEFB) are solid residues generated after harvesting fresh fruit bunches, primarily in major oil palm-producing countries such as Malaysia, Thailand, and Indonesia [1]. As a cost-effective and abundant natural fibre, OPEFB are predominantly found in Malaysia [2]. Recent advancements in biomass valorisation have enabled to the extraction of hemicellulose from OPEFB for hydrogel synthesis, presenting a sustainable approach for material development. Although hemicellulose is the second most abundant natural polymer after cellulose, it remains underutilised as a renewable feedstock. Composed of non-cellulosic heteropolysaccharides with short, branched chains of hexoses and pentoses, hemicellulose can interact with cellulose microfibrils through hydrogen bonding and van der Waals forces. Its structural characteristics, combined with its biocompatibility, biodegradability, and renewability, make it a promising candidate for hydrogel development.

Hydrogels are three-dimensional polymeric networks capable of absorbing and retaining large amounts of water while maintaining structural integrity. Their properties, such as porosity, swelling behaviour, and mechanical stability, are influenced by the crosslinking of hydrophilic polymer chains. The incorporation of crosslinkers is essential for enhancing these properties, enabling application in fields such as biomedical and environmental systems.

In this study, two crosslinkers, N, N'-methylene bisacrylamide (MBA) and glutaraldehyde (GA), were selected due to their distinct crosslinking mechanisms and structural effects on hydrogel networks. N, N'-methylene bisacrylamide, a bifunctional acrylamide derivative, participates in free radical polymerisation by forming covalent bonds between polymer chains, resulting in a rigid and tightly crosslinked network. In contrast, GA, a dialdehyde compound, crosslinks through Schiff base formation and hydrogen bonding,

†Paper presented at the 5th IKMPB Online Symposium: Sustainable Chemistry Innovations Shaping the Future Life

which can introduce flexibility and influence the water uptake behaviour of the hydrogels.

The roles of MBA and GA as crosslinking agents in modifying the chemical and physical properties of hemicellulose-based polymer networks warrants further investigation. Although both have been used in hydrogel synthesis, limited research has directly compared their effects, particularly on the swelling behaviour of hemicellulose-based hydrogels from OPEFB. This knowledge gap limits the ability to tailor OPEFB hydrogels for specific applications. Therefore, this study aims to fill that gap by developing hydrogels using hemicellulose extracted from OPEFB through polymerisation with acrylic acid employing MBA and GA as crosslinking agents. The novelty of this study lies in the direct comparison of the effects of MBA and GA crosslinkers on the structural and functional properties of the hydrogels. Comprehensive characterisation using Fourier transforms infrared spectroscopy (FTIR), X-ray diffraction (XRD), thermogravimetric analysis (TGA), Field emission scanning electron microscopy (FESEM) and swelling behaviour assessment provides valuable insights into optimising hydrogel design for agricultural and environmental applications.

EXPERIMENTAL

Chemicals and Materials

Oil palm empty fruit bunches were collected from Seri Langat Palm Oil Mill Sdn. Bhd. Sodium hydroxide (NaOH, 98%), distilled water, and 95% ethanol were used in the extraction and precipitation of hemicellulose. Hydrochloric acid (HCl, 37%) was used to adjust the solution pH to 5.5. A redox initiation system, comprising sodium sulphite (Na_2SO_3) and potassium persulfate ($K_2S_2O_8$), was employed along with MBA and 50% GA as crosslinking agents while acrylic acid (AA, 99%) served as the monomer. All chemicals were of analytical grade unless otherwise stated. N, N'-methylene bisacrylamide and other reagents were purchased from Chemiz, Malaysia, while GA and AA were obtained from Sigma-Aldrich.

Methodology

Preparation of OPEFB

After being collected, the OPEFB were soaked in water for 24 h and then rinsed with tap water to remove any remaining oil and dirt. The cleaned OPEFB were then subsequently left to dry at room temperature for 24 h. Prior to extraction, the biomass was dried in a Memmert oven (Germany) at 60 °C until a constant weight was achieved to ensure complete moisture removal. The dried biomass was then pulverised using a mechanical grinder (Fritsch Pulverisette 14, Germany) to obtain a fine powder with a particle size of 60 - 120 mesh.

Extraction of Hemicellulose

The Ethos Easy microwave system, equipped with a rotor containing 15 vessels made of modified polytetrafluoroethylene, each with a capacity of 100 mL (SK-15 rotor, Milestone, Sorisole, Italy), was used for the microwave studies. Hemicellulose was extracted from OPEFB using an alkali extraction method with NaOH as the solvent. A loading ratio of 15 mL NaOH per gram of dry biomass was achieved by combining 3 g of dried OPEFB with a specific amount of NaOH to produce pressure vessels. The following parameters were applied for hemicellulose extraction: temperature (130 °C), duration (30 min), and NaOH concentration (10% w/v). The sample mixture was filtered to separate the filtrate from the solid residue. To precipitate the dissolved hemicellulose, the filtrate was neutralised to pH 5.5 using 6 M HCl, followed by the addition of 4 volumes of 95% ethanol. After separating the precipitated hemicellulose, solid hemicellulose was obtained through centrifugation (4500 rpm, 15 min), freeze-drying, and appropriate labelling. All extractions were performed in triplicate.

Preparations of Hemicellulose-based Hydrogel

The first step in hydrogel preparation involved dissolving 0.5 g of purified hemicellulose in 10 mL of distilled water in a beaker. The mixture was stirred and placed in a water bath set to 90 °C for 1 h. Subsequently, the redox initiator system, consisting of 0.04 g of Na_2SO_3 and 0.01 g of $K_2S_2O_8$, was added to the beaker under magnetic stirring for 10 min. Following this, 5 g of AA was introduced. N, N'-methylene bisacrylamide and glutaraldehyde, which served as crosslinking agents, were then added to the solution mixture and stirred using a magnetic stirrer for 10 min. Different amounts of MBA and GA (0.01, 0.05, and 0.10 g) were used in this process. After the addition of the crosslinking agents, the reaction proceeded for 15 min in the water bath at 90 °C. Subsequently, the resulting hydrogel product was dried in a vacuum dryer at 40 °C until a constant mass was reached. All hydrogel preparations were performed in triplicate.

Swelling Behaviour Analysis

The evaluation of water absorption ability involved measuring the weights of sectioned dried hydrogel samples before and after immersion in distilled water. The samples were immersed in distilled water at room temperature for 48 h. After the immersion period, the samples were extracted, and excess water was removed using filter paper before recording the final weight. The swelling behaviour of the hydrogels was analysed in triplicate. The swelling percentage was determined using Equation 1.

$$Swelling\ (\%) = \frac{Ws - Wd}{Wd}\ x\ 100\% \qquad \text{Equation 1}$$

Where W_s is the weight of the swollen material and W_d is the weight of the dry material.

Characterisation

Fourier Transforms Infrared Spectroscopy

Fourier transform infrared spectroscopy was used to identify functional groups in the hydrogel, providing insights into its chemical structure. After complete drying, the OPEFB, hemicellulose, and hydrogel were each separately ground with potassium bromide into fine powders using an agate mortar prior to analysis. The resulting mixture was pressed into a pellet and scanned using an infrared spectrometer over the range of 400 - 4000 cm^{-1}.

X-ray Diffraction

The crystalline structure of the hydrogels was characterised by grinding a dried hydrogel sample into a fine powder and placing it on the sample holder of an X-ray diffractometer, weighing approximately 1 g. The analysis was performed at a scan rate of 2°/min over a 2θ range of 5°- 80°. The resulting diffraction patterns were used to identify the crystalline phases.

Thermogravimetry Analysis

A TGA analysis of dried hydrogel samples required between 5–10 mg of the hydrogel material, which was weighed before being placed into the TGA equipment. The hydrogel sample was heated from room temperature to 600 °C at a constant heating rate of 10 °C/min under nitrogen conditions. These analyses provided vital insights into the thermal behaviour and structural stability of the hydrogels, which were significantly influenced by the density and type of crosslinking.

Field Emission Scanning Electron Microscopy

The treated samples were analysed using a field emission scanning electron microscope (Zeiss, Merlin) at an acceleration voltage of 30 kV and 1.6 nm. Prior to analysis, an iridium coating was applied to the samples using an ion sputter coater.

RESULTS AND DISCUSSION

Formation of Hydrogels

The structural characteristics of GA-crosslinked hydrogels, as illustrated in Figure 1, exhibited a distinct trend in morphological changes with increasing GA amount. Crosslinking with GA influences network compactness, flexibility, and water retention by modulating the density of covalent bonds formed between hemicellulose chains. At 0.01 g of GA, the hydrogel displayed a soft, highly swollen, and loosely structured morphology, indicating the formation of a weakly crosslinked network. The high swelling suggests excessive water absorption due to insufficient crosslinking density, which limited the formation of a stable gel network. Similar findings have been reported, where low GA amounts (≤ 0.027 g of GA/g polymer) resulted in hydrogels with poor mechanical strength and unstable structures [3]. A noticeable increase in hydrogel density and opacity was observed at 0.05 g GA, where crosslinking enhanced polymeric stability. The hydrogel becomes more compact, with a denser matrix structure, correlating with increased crosslinking efficiency. However, small regions of visible aggregation suggested incomplete crosslinking, possibly due to the inhomogeneous distribution of GA molecules during gel formation. At 0.10 g GA, the hydrogel transformed into a highly rigid and compact structure, displaying minimal water retention. This higher GA amount resulted in over-crosslinking, thus restricting polymer chain mobility, and producing a less porous and denser gel network [4]. Captured trends indicated that higher GA amounts yield stiffer hydrogel networks. [5] reported that increased GA content resulted in enhanced tensile strength but reduced flexibility, supporting the observed structural densification at 0.10 g GA. Consequently, GA crosslinking optimises hydrogel stability, making it particularly suitable for applications requiring controlled swelling and structural resilience.

Hydrogels synthesised using MBA crosslinking exhibit morphological changes that depends on the amount of the crosslinker, as shown in Figure 1. The use of MBA in the crosslinking process facilitates free-radical-initiated polymerisation, producing extensive hydrogel networks. At an MBA amount of 0.01 g, the hydrogel forms a thin layer with easy spreadability and a uniform appearance. This polymer matrix extends widely across the network due to its low interlinking density. Research has shown that weak crosslinking occurs at low MBA amounts used, leading to increased swelling capacity [6]. At 0.05 g MBA, the gel thickness increased, and its colour darkened, accompanied by a more well-defined structural formation due to improved crosslinking. The polymer network becomes more stable while absorbing less water. However, structural variations at specific points indicate the possibility of uneven crosslinking, likely caused by irregular polymer distribution during gelation. When the MBA amounts reached 0.10 g, the hydrogel exhibited an unexpectedly solid structure, differing from the typical properties of MBA-crosslinked hydrogels. Studies have shown that MBA-based hydrogels generally produce elastic and highly absorbent materials [7]. However, excessive crosslinking at high MBA amounts leads to the formation of compact polymeric networks, which reduce the swelling capacity of the hydrogel [8]. The data indicate that hydrogel stiffness increases with higher MBA amounts. According to [9], MBA amounts exceeding 0.10 g result in excessive crosslinking, reducing water retention and making the hydrogel more brittle. Optimising MBA crosslinking is essential, as it directly influences the hydrogel's ability to maintain structural integrity while allowing expansion and providing suitable flexibility for various applications.

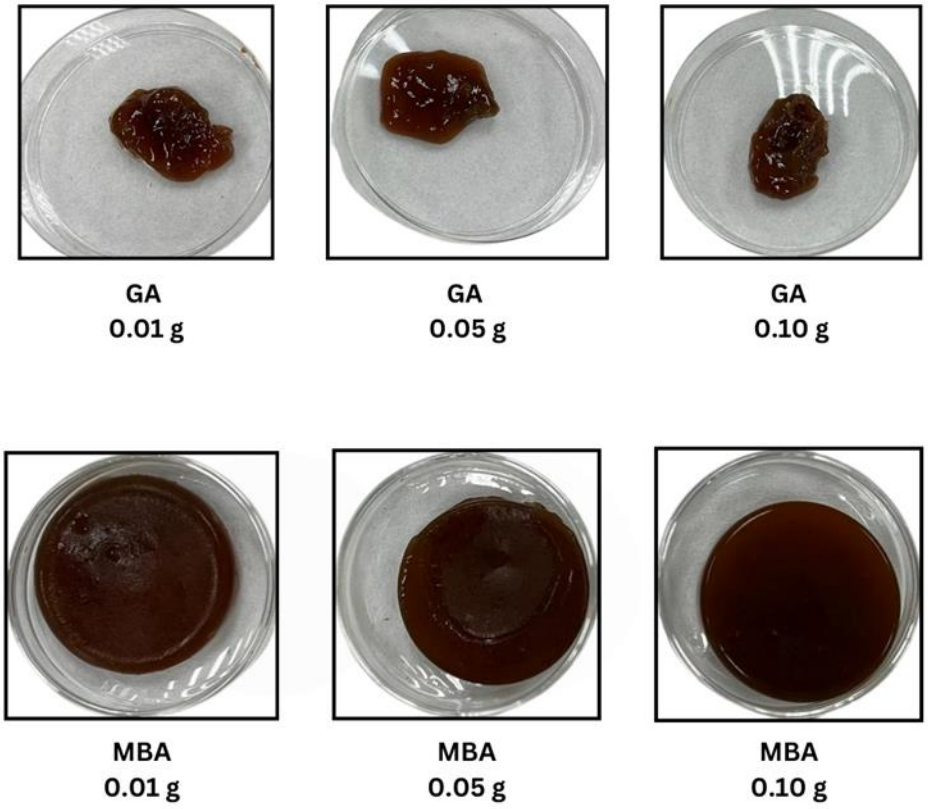

Figure 1. Physical appearance of hemicellulose-based hydrogels crosslinked with varying amounts of GA and MBA.

Table 1. Swelling behaviour of hydrogels crosslinked with varying amounts of MBA and GA.

Crosslinker	Amount (g)	Wd (g)	Ws (g)	Swelling Ratio	Swelling (%)
MBA	0.01	1.8845 ± 0.0463	13.4651 ± 0.2450	6.15 ± 0.13	615 ± 13
	0.05	1.1363 ± 0.0392	7.3648 ± 0.1818	5.48 ± 0.16	548 ± 16
	0.10	2.0735 ± 0.1779	7.1762 ± 0.3110	2.46 ± 0.15	246 ± 15
GA	0.01	1.4025 ± 0.1989	2.3678 ± 0.0561	0.69 ± 0.04	69 ± 4
	0.05	0.7692 ± 0.0754	2.0278 ± 0.0769	1.64 ± 0.10	164 ± 10
	0.10	0.4655 ± 0.1190	0.9341 ± 0.0605	1.01 ± 0.13	101 ±13

W_d= Weight of dry material, W_s= weight of swollen material

Swelling Behaviour

Research on MBA-crosslinked hydrogels revealed that higher crosslinker amounts resulted in lower swelling ratios (Table 1). Hydrogels crosslinked with the minimal MBA amounts of 0.01 g exhibited a swelling ratio of 6.15, corresponding to a swelling percentage of 615%. The less compact structure of these crosslinked networks allows water molecules to penetrate more deeply and interact with the hydrophilic backbone of hemicellulose. In contrast, when the MBA amount was increased to 0.10 g, the swelling ratio decreased to 2.46 (246%), demonstrating how a denser network restricts water diffusion, thereby reducing hydrogel flexibility [10].

The distinct trend of GA-crosslinked hydrogels, as presented in Table 1, shows noticeable differences in swelling behaviour. When using only 0.01 g of GA, the swelling ratio was 0.69, corresponding to a swelling percentage of 69%, indicating the formation of a dense network from the outset. Swelling

ratios for GA-crosslinked hydrogels at GA amounts of 0.05 g and 0.10 g were measured at 1.64 and 1.01, equivalent to swelling percentages of 164% and 101%, respectively. Unlike MBA, GA allows for a more moderate and controllable network structure, balancing density and flexibility to retain more water. [11, 12]. Research findings highlight that both the type and amount of the crosslinker fundamentally influence the mechanical properties of hydrogel materials. Higher MBA amounts result in stiffer networks, leading to a significant decrease in swelling behaviour. Such rigid and compact networks are potentially suited for load-bearing or structural applications where dimensional stability is critical. In contrast, GA-crosslinked hydrogels form balanced networks that allow moderate swelling, making them more appropriate for high-absorption applications such as agricultural moisture-retaining pads or biomedical wound dressings where flexibility and water uptake are desirable.

Characterisation

Fourier Transform Infrared Spectroscopy

The MBA-crosslinked hydrogels exhibited distinct FTIR signatures, as presented in Figure 2. Absorption peaks were observed between 3426 and 3443 cm^{-1} in the O-H/N-H stretching region, while C=O stretching appeared at 1651–1652 cm^{-1}, alongside C-N stretch bands between 1409 and 1427 cm^{-1}. The identification of these FTIR peaks confirms the formation of amide bonds through MBA crosslinking, resulting in hydrogel matrices with increased stiffness and reduced swelling capacity. The FTIR measurements of MBA-crosslinked hydrogels produced spectral patterns consistent with those reported in [13]. Additionally, the findings aligned with those of [14], which highlighted enhanced mechanical properties and controlled swelling behaviour at higher MBA amounts.

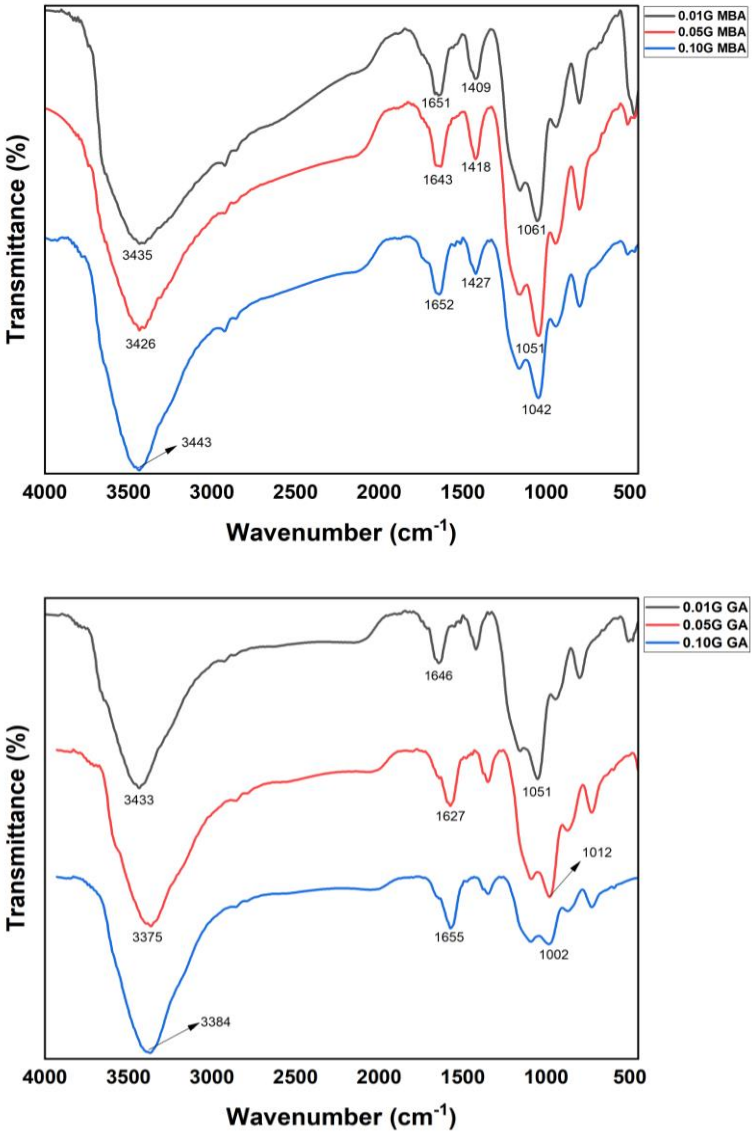

Figure 2. FTIR spectra of hydrogels crosslinked with varying amounts of MBA and GA.

The FTIR spectra of GA-crosslinked hydrogels, as shown in Figure 2, exhibit major absorption peaks at 3375–3433 cm^{-1} (O-H stretching), 1627–1646 cm^{-1} (C=O stretching), and 1002–1051 cm^{-1} (C-O stretching). These absorption peaks indicate both hydrogen bonding and the successful formation of acetal bridges between the aldehyde functional groups of GA and the hydroxyl groups of hemicellulose. This interaction confirms the development of a tightly crosslinked network structure, enhancing the structural integrity of the hydrogel and making it suitable for applications requiring pH-responsive behaviour. Similar FTIR results from studies on hemicellulose-based hydrogels by Sun et al., Mansur et al., and Peng et al. demonstrate that GA crosslinking improves hydrogel stability and adaptability for specialised applications, such as wound care and drug delivery systems [15,16]. The FTIR results also confirm successful crosslinking in both MBA- and GA- based hydrogels. N, N'-methylene bisacrylamide forms amide bonds, providing greater rigidity to the hydrogel, while GA forms acetal bridges, creating a more flexible structure suited for specific applications.

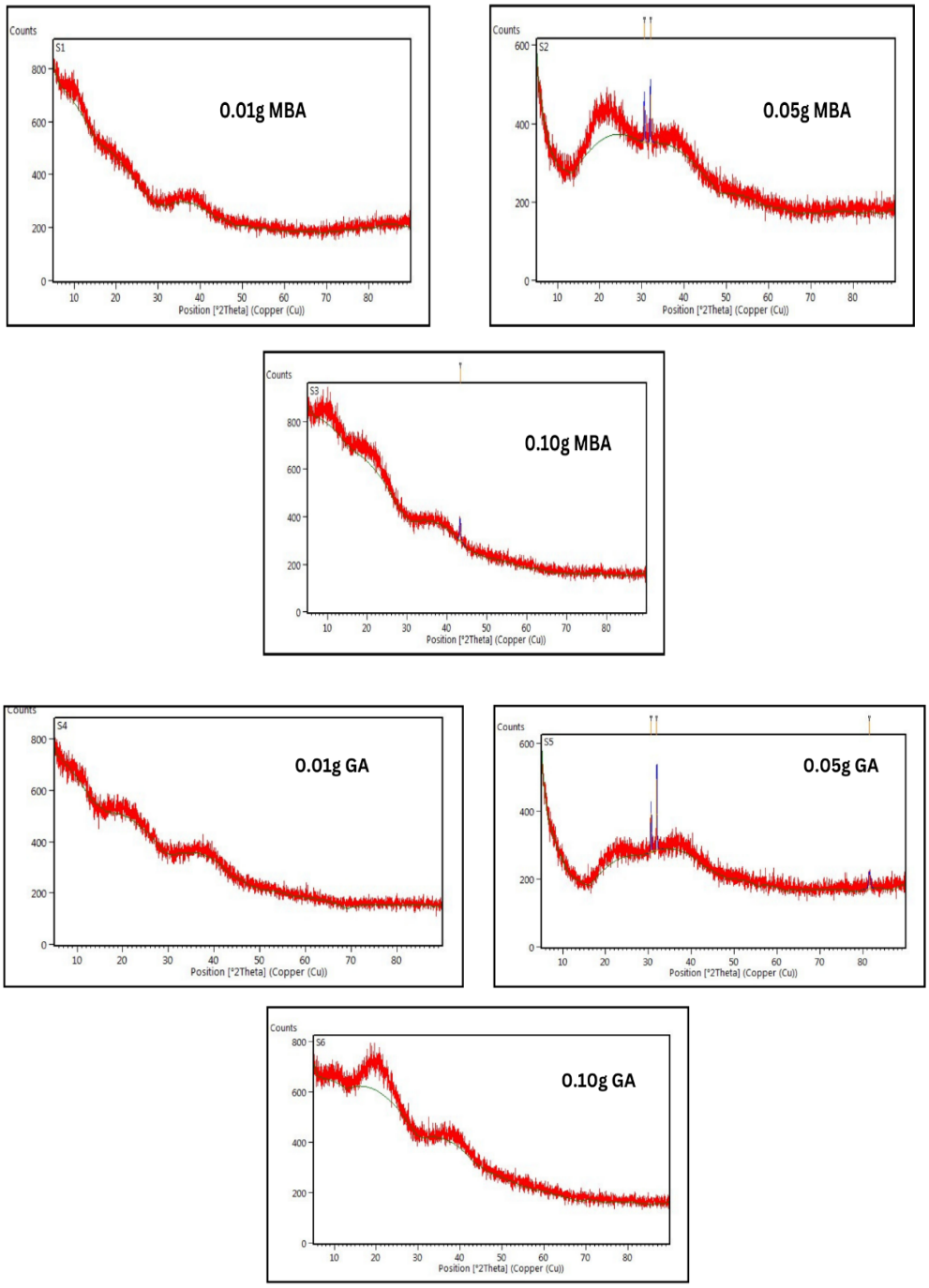

Figure 3. XRD spectra of hydrogels crosslinked with varying amounts of MBA and GA.

X-Ray Diffraction

The MBA-crosslinked hydrogels display broad 2θ peaks ranging from 10° to 80°, indicating a predominantly amorphous structure. Increasing the MBA amounts from 0.01 g to 0.10 g resulted in stronger peaks, primarily at angular positions of 22° and 30°, suggesting the formation of semi-crystalline structures (Figure 3). These observations reflect structural stiffening and the development of semi-crystalline domains in semi-IPN hydrogels crosslinked by MBA, as documented by [17]. Additionally, [18] reported that higher MBA amounts enhance crosslink density and facilitate crystalline domain formation, a finding further confirmed by [19] in hydrogel structures. Large peaks in the 10°- 80° range also appear in the XRD spectra of GA-crosslinked hydrogels (Figure 3), indicating that these hydrogels primarily exhibit amorphous structures. Increasing the GA content from 0.01 g to 0.10 g results in higher spectral peak intensities, reflecting improved crosslinking and a structural transition towards semi-crystalline patterns due to lignin involvement. Lignin-infused hydrogels demonstrate enhanced structural integrity, as reported by [20], while [21] described lignin-based hydrogels as capable of forming semi-crystalline structures that contribute to greater stability. The XRD analysis demonstrates that both MBA and GA influence the structural organisation of hydrogels, with increasing crosslinker content leading to a partial shift from amorphous to semi-crystalline patterns. These structural changes suggest improved stability and mechanical strength, particularly in lignin-containing networks.

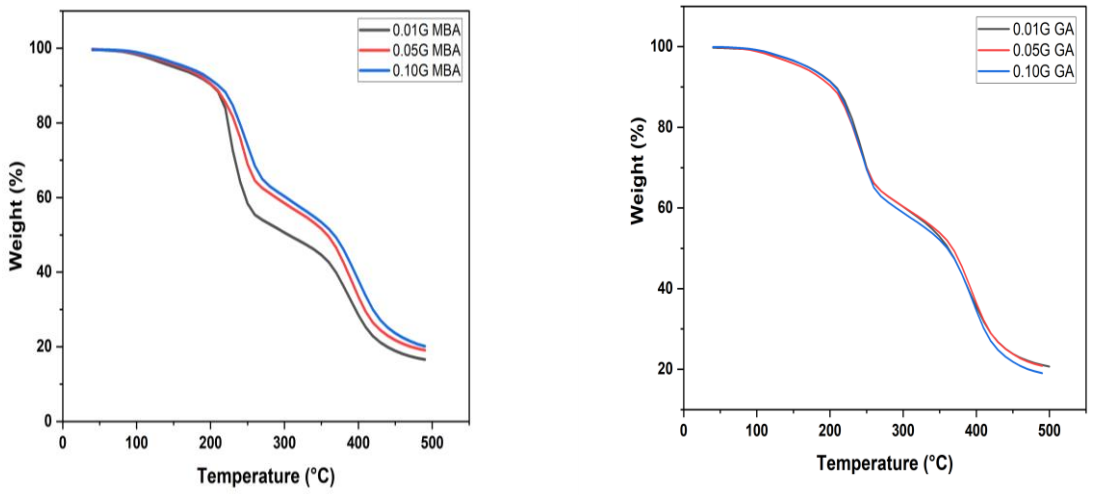

TGA curves

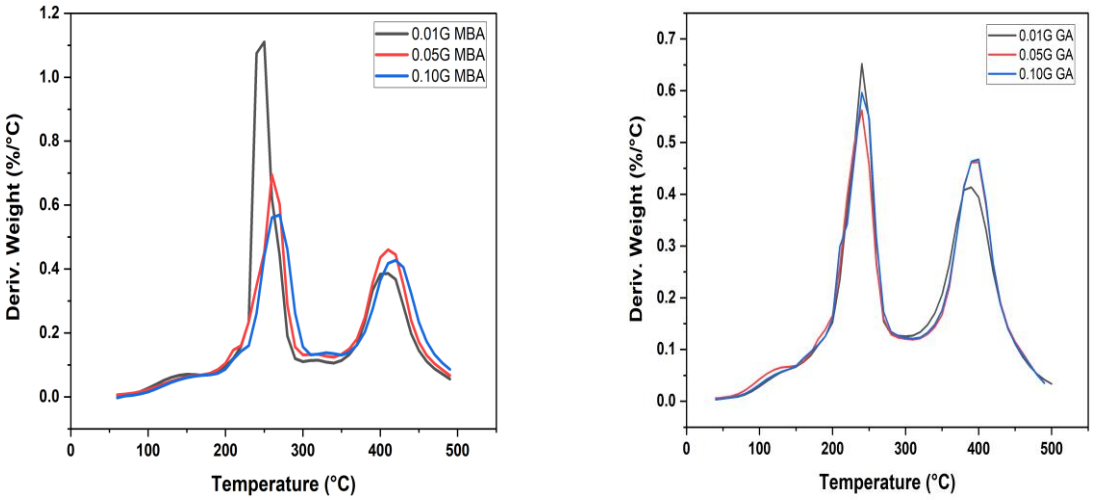

DTG curves

Figure 4. TGA and DTG curves of hemicellulose-based hydrogels crosslinked with varying amounts of MBA and GA.

Thermogravimetric Analysis

The initial phase of weight loss in the TGA curve of MBA-crosslinked hydrogels corresponds to the evaporation of water molecules from the network, including loosely bound water. The TGA data for all MBA sample amounts indicate stable hydrophilic characteristics, along with consistent decomposition of hemicellulose and amide structures (Figure 4).

Increasing the amount of MBA enhanced the thermal stability of hemicellulose-based hydrogels, as evidenced by a progressive shift in peak degradation temperature (Tmax) from 240 °C at 0.01 g MBA to 255 °C at 0.10 g. This trend indicates that higher MBA content promotes the formation of a more robust crosslinked network that resists thermal decomposition. Correspondingly, total weight loss decreases from 82% to 80% as MBA amount increases, supporting the conclusion that stronger crosslinking limits mass loss during heating. The DTG curves presented in Figure 4 display two distinct thermal degradation peaks. The first peak, occurring between 200°C and 250°C, corresponds to the breakdown of smaller organic molecules, while the second peak, occurring near 255°C, reflects the decomposition of the main crosslinked polymer matrix. Reduced peak intensity and delayed degradation at higher MBA amounts further confirm improved material stability through increased crosslink density, as also reported by previous studies [22,23].

Figure 4 also illustrates that hydrogels crosslinked with GA, the initial degradation temperature remains relatively constant at 170-175°C across all amounts, suggesting similar initial thermal behaviour. Hydrogel with 0.01 g and 0.10 g of GA exhibit similar initial weight loss, indicating comparable water-holding capacity and hydrophilic properties. However, an increase in GA amount does not lead to a corresponding improvement in thermal resistance. In fact, Tmax slightly decreases from 235°C at 0.01 g GA to 228°C at 0.10 g, and total weight loss slightly increases from 82% to 83%. This trend suggests that while GA does provide crosslinking through acetal bond formation with hemicellulose excessive GA may not significantly enhance and may even slightly reduce thermal stability. The DTG curves in Figure 4 display two prominent degradation peaks: the first peak, between 200°C and 250°C, corresponds to the decomposition of unstable hemicellulose units and minor organic compounds, while the second, broader peak near 230°C corresponds to the decomposition of the GA-crosslinked network. Increasing GA levels slightly shift the degradation profile and reduce peak intensity, which may still indicate some improvement in crosslinking uniformity [24,25]. Table 2 shows a summary of TGA results for MBA- and GA- crosslinked hydrogels. These thermal analyses demonstrate that both MBA and GA enhance the thermal stability of hydrogels by increasing crosslinking density. N, N'-methylene bisacrylamide leads to higher thermal resistance and reduced degradation, while GA imparts comparable stability through acetal bonding, suggesting suitability for applications requiring heat resilience and moisture retention.

Field Emission Scanning Electron Microscopy

Hydrogels synthesised with varying amounts of MBA and GA, exhibit distinct differences in surface morphology, highlighting the impact of crosslinker amount on hydrogel properties. Figure 5 presents FESEM images of hydrogels crosslinked with different amounts of GA and MBA, captured at 800× magnification. These images provide insights into surface texture, porosity, and network formation variations between the two crosslinkers. As shown in Figure 5, the GA-crosslinked hydrogel at the lowest amount (0.01 g) exhibits a rough and porous surface, indicating a loosely crosslinked polymer network. The pronounced porosity suggests a high swelling potential, as the open structure allows for greater water absorption. Similarly, Figure 5 reveals that the MBA-crosslinked hydrogel at 0.01 g displays an uneven surface with noticeable protrusions. However, the pore interconnectivity appears higher than in the GA-crosslinked hydrogel. This variation may be attributed to the distinct crosslinking mechanisms of the two agents where GA forms covalent bonds with hydroxyl groups, whereas MBA primarily engages in radical polymerisation with acrylamide-based structures [26].

Increasing the crosslinker amount up to 0.05 g, resulted in hydrogels crosslinked with both GA and MBA, showing a denser structure with lower porousity as seen in Figure 5. The structure of GA-crosslinked hydrogels appears more rigid with fewer voids indicating that the crosslink density increases significantly among the networks. Conversely, the conditioned MBA-crosslinked hydrogel demonstrates not only decreased porosity, but also maintains a more open network than its GA counterpart. This suggests that MBA-crosslinked hydrogels exhibit a degree of flexibility at higher amounts of crosslinkers, which may make these networks more favourable for use in applications that depend on controlled swelling and mechanical adaptability [27. 28]. At the crosslinkers amount of 0.10 g, the GA-crosslinked hydrogel in Figure 5 has a very compact and smooth structure with little visible porosity. This is indicative of excessive crosslinking, leading to brittleness and loss of swelling ability. Although the 0.10 g MBA-crosslinked hydrogel shows an overall much denser structure, it retains some level of porosity. This means that MBA provides more uniform crosslinking, and does not over-rigidise while still improving the mechanical properties [29]. The FESEM results show that GA makes the hydrogel surface more compact and rigid as its amount increases, while MBA helps maintain some porosity and flexibility. This means that MBA may be better for applictions that require both strength and swellability.

Table 2. Summary of TGA analysis for MBA- and GA-crosslinked hydrogels.

Crosslinker	Amount (g)	Initial Degradation Temp (°C)	Tmax (°C)	Residual Weight (%)	Weight Loss (%)
MBA	0.01	170	240	18	82
	0.05	180	250	19	81
	0.10	185	255	20	80
GA	0.01	170	235	18	82
	0.05	170	230	18	82
	0.10	175	228	17	83

Tmax=Maximum degradation temperature

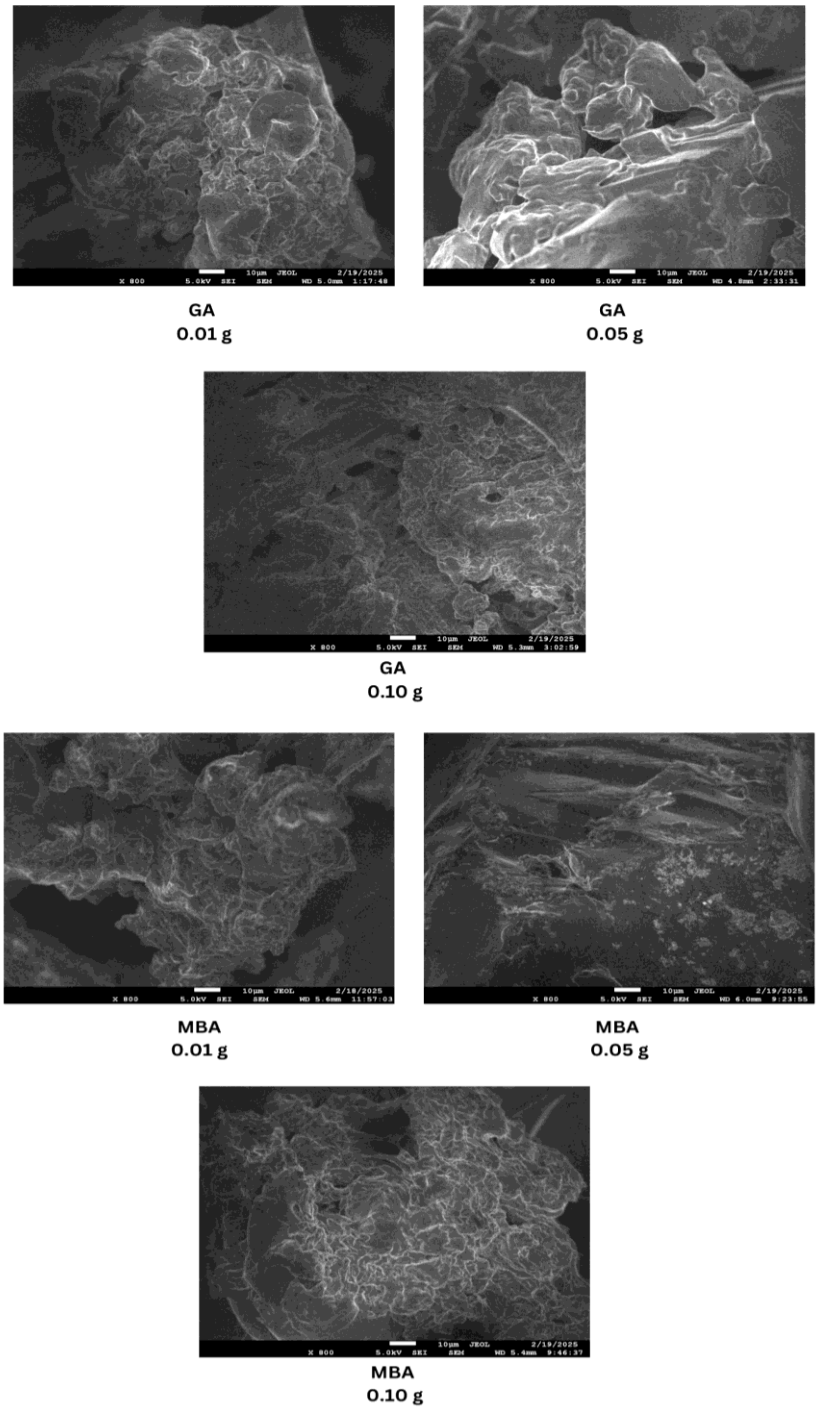

Figure 5. FESEM images of hydrogels crosslinked with varying amounts of GA and MBA.

CONCLUSION

This study successfully developed GA- and MBA-crosslinked hemicellulose-based hydrogels, highlighting their potential for various applications. Glutaraldehyde-crosslinked hydrogels demonstrated high flexibility and water absorption due to acetal bridge formation, making them suitable for applications requiring high swelling capacity and controlled water release, such as agricultural water retention materials, wound dressings, and drug delivery systems. In contrast, MBA-crosslinked hydrogels formed stronger, more rigid networks, resulting in enhanced thermal stability but lower swelling capacity. These characteristics make MBA-crosslinked hydrogels more appropriate for packaging, biomedical scaffolds, or adsorbents in harsh environments. Fourier transform infrared spectroscopy analysis confirmed the presence of significant structural bonds, while XRD revealed that GA-crosslinked hydrogels remained mostly amorphous, whereas MBA-crosslinked hydrogels developed semi-crystalline structures. Thermal analysis indicated that increasing crosslinker content improved thermal resistance, which is beneficial for thermal processing or sterilisation in biomedical and food applications. The FESEM images revealed that GA-crosslinked hydrogels exhibited porous structures at low crosslinker amounts, while MBA-crosslinked hydrogels became denser and more compact with increasing crosslinker content. This study demonstrates that the type and amount of crosslinker significantly influence the swelling behaviour and structural properties of hemicellulose-based hydrogels derived from OPEFB.

ACKNOWLEDGEMENTS

The authors are grateful to the Ministry of Higher Education for the financial support provided for this research under grant number FRGS/1/2022/STG04/UITM/02/10.

REFERENCES

1. Akita, H., Yusoff, M. Z. M. and Fujimoto, S. (2021) Preparation of oil palm empty fruit bunch hydrolysate. *Fermentation*, **7(2)**, 81.

2. Padzil, F. N. M., Lee, S. H., Ainun, Z. M. A., Lee, C. H. and Abdullah, L. C. (2020) Potential of oil palm empty fruit bunch resources in nanocellulose hydrogel production for versatile applications: A review. *Materials*, **13(5)**, 1245.

3. Distantina, S., Fahrurrozi, M. and Wiratni, W. (2013) Effect of Crosslinker Concentration on the Physical Properties of Hemicellulose-Based Hydrogels. *Journal of Polymers and the Environment*, **21(4)**, 987–995.

4. Mirzaei, B. E., Ramakrishna, S. and Moghaddam, A. D. (2013) Engineering Hydrogels as Extracellular Matrix Mimics. *Nanomedicine*, **8(4)**, 591–625.

5. Musa, A. and Hameed, K. H. (2021) Properties of Crosslinked Hydrogels: A Review. *Polymer Bulletin*, **78(6)**, 3663–3689.

6. Pourjavadi, A., Barzegar, S. and Mahdavinia, G. R. (2004) Modified Chitosan. IV. Superabsorbent Hydrogels from Poly(acrylic acid-co-acrylamide) Grafted onto Chitosan with Higher Efficiency Cationic Dye Adsorption Capacity. *European Polymer Journal*, **40(6)**, 1399–1407.

7. Mansur, H. S., Sadahira, C. M., Souza, A. N. and Mansur, A. A. P. (2008) FTIR Spectroscopy Characterization of Poly(vinyl alcohol) Hydrogel with Different Hydrolysis Degree and Chemically Crosslinked with Glutaraldehyde. *Materials Science and Engineering C*, **28(5)**, 539–548.

8. Kabiri, K., Omidian, H., Hashemi, S. A. and Zohuriaan-Mehr, M. J. (2003) Superabsorbent Hydrogel Composites and Nanocomposites: A Review. *Polymer Composites*, **24(1)**, 85–101.

9. Zhang, Q., Yu, Q., Zheng, H. and Ning, Z. (2018) Crosslinked Polymeric Networks for Low-Moisture-Content Hydrogel Applications. *Journal of Materials Chemistry B*, **6(10)**, 1593–1600.

10. Rahman, F., Rafiquee, M. Z. A., Aazam, E. S., Iqubal, S. M. S., Khan, A. A., Mohammed, T., Maqbul, M. S., Dawoud, A., Khan, K. A. and Ikbal, A. R. (2020) Effects of Cross-linker Variation on Swelling Behavior of Hydrogels. *Asian Journal of Pharmaceutics*, **14(3),** 351–355.

11. Collins, M. and Birkinshaw, C. (2008) Investigation of the swelling behavior of crosslinked hyaluronic acid films and hydrogels produced using homogeneous reactions. *Journal of Applied Polymer Science*, **109**, 923–931.

12. Kumari, R. and Shekhar, S. (2023) Effect of crosslinking on thermodynamics interactions and network parameters of terpolymeric hydrogels. *Journal of Macromolecular Science, Part B*, **62(12)**, 689–717.

13. Mandal, B. and Ray, S. K. (2013) Synthesis of interpenetrating network hydrogel from poly (acrylic acid-co-hydroxyethyl methacrylate) and sodium alginate: Modeling and kinetics study for removal of synthetic dyes from water. *Carbohydrate Polymers*, **98(1)**, 257–269.

14. Pourjavadi, A., Barzegar, Sh. and Mahdavinia, G. R. (2006) MBA-crosslinked Na-Alg/CMC as a smart full-polysaccharide superabsorbent hydrogels. *Carbohydrate Polymers*, **66(3)**, 386–395.

15. Sun, X. -F., Wang, H. -H., Jing, Z. -X. and Mohanathas, R. (2012) Hemicellulose-based pH-sensitive and biodegradable hydrogel for controlled drug delivery. *Carbohydrate Polymers*, **92(2)**, 1357–1366.

16. Peng, X. -W., Ren, J. -L., Zhong, L. -X., Peng, F. and Sun, R. -C. (2011) Xylan-rich Hemicelluloses-graft-Acrylic Acid Ionic Hydrogels with Rapid Responses to pH, Salt, and Organic Solvents. *Journal of Agricultural and Food Chemistry*, **59(15)**, 8208–8215.

17. Samanta, H. S. and Ray, S. K. (2013) Synthesis, characterization, swelling and drug release behavior of semi-interpenetrating network hydrogels of sodium alginate and polyacrylamide. *Carbohydrate Polymers*, **99**, 666–678.

18. Mishra, S., Bajpai, R., Katare, R. and Bajpai, A. K. (2007) Radiation induced crosslinking effect on semi-interpenetrating polymer networks of poly(vinyl alcohol). *Express Polymer Letters*, **1(7)**, 407–415.

19. Deshpande, D. S., Bajpai, R. and Bajpai, A. K. (2012) Synthesis and characterization of polyvinyl alcohol based semi interpenetrating polymeric networks. *Journal of Polymer Research*, **19(8)**, 9938.

20. Ciolacu, D., Doroftei, F., Cazacu, G., Cazacu, M., Ghica, G. and Alley, V. (2013) Morphological and surface aspects of cellulose-lignin hydrogels. *Cellulose Chemistry and Technology*, **47(5-6)**, 377–386.

21. Morales, A., Labidi, J. and Gullón, P. (2019) Assessment of green approaches for the synthesis of physically crosslinked lignin hydrogels. *Journal of Industrial and Engineering Chemistry*, **81**, 475–487.

22. Saragih, S. W., Wirjosentono, B., Eddiyanto, N. and Meliana, Y. (2020) Influence of crosslinking agent on the morphology, chemical, crystallinity and thermal properties of cellulose nanofiber using steam explosion. *Case Studies in Thermal Engineering*, **22**, 100740.

23. Dhanapal, V., Subhapriya, P., Nithyanandam, K. P., Kiruthika, M. V., Keerthana, T. and Dineshkumar, G. (2020) Design, synthesis and evaluation of N,N1-methylenebisacrylamide crosslinked smart polymer hydrogel for the controlled release of water and plant nutrients in agriculture field. *Materials Today Proceedings*, **45**, 2491–2497.

24. Gliko-Kabir, I., Penhasi, A. and Rubinstein, A. (1999) Characterization of crosslinked guar by thermal analysis. *Carbohydrate Research*, **316(1–4)**, 6–13.

25. Mansur, H. S., Sadahira, C. M., Souza, A. N. and Mansur, A. A. P. (2007) FTIR spectroscopy characterization of poly (vinyl alcohol) hydrogel with different hydrolysis degree and chemically crosslinked with glutaraldehyde. *Materials Science and Engineering C*, **28(4)**, 539–548.

26. Hiremath, J. N. and Vishalakshi, B. (2012) Effect of Crosslinking on swelling behaviour of IPN hydrogels of Guar Gum and Polyacrylamide. *Der Pharma Chemica*, **4(3)**, 946–955.

27. Saragih, S. W., Wirjosentono, B., Eddiyanto, N. and Meliana, Y. (2020) Influence of crosslinking agent on the morphology, chemical, crystallinity and thermal properties of cellulose nanofiber using steam explosion. *Case Studies in Thermal Engineering*, **22**, 100740.

28. Zhang, Q., Liu, X., Ren, X., Duan, L. and Gao, G. (2018) Adenine-mediated adhesive and tough hydrogel based on hybrid crosslinking. *European Polymer Journal*, **106,** 139–147.

29. Dmitriev, I., Kuryndin, I., Bobrova, N. and Smirnov, M. (2015) Swelling behavior and network characterization of hydrogels from linear polyacrylamide crosslinked with glutaraldehyde. *Materials Today Communications*, **4**, 93–100.